

CONF-8404124--8

UCRL--90866

DE84 012956

Review of Ultraviolet Damage Threshold  
Measurements at Lawrence Livermore  
National Laboratory

W. Howard Lowdermilk  
and  
David Milam

This paper was prepared for submittal to  
SPIE Technical Symposium East '84  
Arlington, Virginia  
April 29-May 4, 1984

May 30, 1984

Lawrence  
Livermore  
National  
Laboratory

This is a preprint of a paper intended for publication in a journal or proceedings. Since changes may be made before publication, this preprint is made available with the understanding that it will not be cited or reproduced without the permission of the author.

**NOTICE**  
**ALL RIGHTS OF THIS REPORT ARE ILLEGIBLE**  
This report has been reproduced from the best available copy to permit the broadest possible availability.

**MASTER**

DISTRIBUTION OF THIS DOCUMENT IS UNLIMITED

## **DISCLAIMER**

This report was prepared as an account of work sponsored by an agency of the United States Government. Neither the United States Government nor any agency thereof, nor any of their employees, makes any warranty, express or implied, or assumes any legal liability or responsibility for the accuracy, completeness, or usefulness of any information, apparatus, product, or process disclosed, or represents that its use would not infringe privately owned rights. Reference herein to any specific commercial product, process, or service by trade name, trademark, manufacturer, or otherwise does not necessarily constitute or imply its endorsement, recommendation, or favoring by the United States Government or any agency thereof. The views and opinions of authors expressed herein do not necessarily state or reflect those of the United States Government or any agency thereof.

Review of ultraviolet damage threshold measurements at  
Lawrence Livermore National Laboratory

W. Howard Lowdermilk and David Milan

Lawrence Livermore National Laboratory  
Mail Stop L-490, P.O. Box 5508, Livermore, California 94550

Abstract

The results of damage threshold measurements made at LLNL using ultraviolet wavelength laser pulses are reviewed. Measurements were made with pulses from a krypton fluoride laser with wavelength of 248 nm and pulse duration of 20 ns and with Nd-glass laser pulses converted to the third harmonic wavelength of 355 nm with duration of 0.6 ns. Measurements are presented for transparent window materials, crystals for harmonic generation, single layer dielectric films of oxide and fluoride materials and multilayer high reflectivity and antireflective coatings.

Introduction

Potential applications of high-power, pulsed, UV lasers in such areas as laser communications and inertial confinement fusion have stimulated studies of damage resistance in bulk materials and thin film coatings for ultraviolet wavelengths and development of improved materials. Work of this nature has been in progress at Lawrence Livermore National Laboratory (LLNL) since 1980. During this time, numerous tests have been conducted on materials intended for use at the 248 nm wavelength of krypton fluoride lasers and at the 355 nm, third-harmonic wavelength of Nd-doped glass or crystalline host lasers. This paper summarizes the data from these experiments. For a more detailed description of each experiment, the original references should be consulted.

In the following sections we review the apparatus and experimental methods used to measure damage thresholds, the results obtained from measurements at 248 nm using 20 ns duration pulses and at 355 nm using 0.6 ns pulses and finally the limited data available on the variation in damage thresholds as a function of pulse duration from 0.6 ns to 70 ns at 355 nm wavelength.

All experiments on thin film coatings were a joint effort by Optical Coating Laboratory, Inc. (OCLI) and LLNL. Coatings were deposited by OCLI. Damage threshold measurements were made at LLNL and other measurements of physical and optical properties of the coatings were made at OCLI.

The data reviewed in this paper represent the current state of ongoing materials development and testing. It is premature to draw definite conclusions about the ultimate potential of the materials, surface preparation techniques or coating deposition methods.

Experimental procedures

Threshold measurements reviewed here were made with 20 ns, 248 nm pulses from a KrF laser, or with 355 nm pulses produced by third harmonic generation of 1064 nm pulses from a Nd-glass laser. Crystals of potassium dihydrogen phosphate (KDP) were used for the harmonic generation process. The experimental arrangement for the measurement of damage thresholds is illustrated in Fig. 1. The incident beam was focused by a lens with focal length of 4-6 m. The sample was placed upstream of the beam waist at a position where the beam diameter was 1-3 mm. The focused beam was divided to form diagnostic beams which were directed into a calorimeter, which measured the laser pulse energy, and to one or more devices which recorded the intensity distribution of the pulse. All diagnostics and the damage test sample were placed equidistant from the focusing lens, so the beams incident on the diagnostic devices were identical in size and shape to the beam incident on the sample.

The fluence distribution in the focused 355 nm beam was uniform and centrosymmetric, but the shape of the beam varied with beam intensity due to nonlinearities in gain saturation of laser amplifiers and in harmonic conversion. The fluence distribution for each shot was recorded by a silicon vidicon. Peak fluence in the distribution was computed by normalizing the fluence distribution so that its integral agreed with the measured pulse energy. Integration was done numerically, and was therefore insensitive to the exact shape of the beam, provided that the beam was large relative to the 80  $\mu$ m

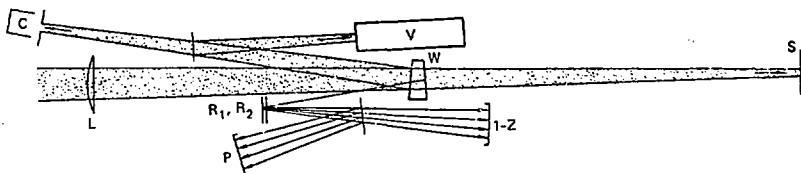


Figure 1. Laser damage experiment. Beam was focused by lens (L) with focal length of 4-6 m onto the sample(s). Diagnostic beams reflected from the surfaces of the wedged splitter (W) were incident on a calorimeter (C), a vidicon camera (V), and onto both Polaroid film and Kodak 1-z emulsions.

spatial resolution of the vidicon. Fluence measurements at 355 nm are typically accurate to  $\pm 5\%$ .

In 248 nm experiments, the beam incident on the sample was 2 mm in diameter at  $e^{-2}$  in intensity, but the fluence distribution contained smaller diameter regions of higher intensity. Fluence in these hot spots was constant to within 5% over areas not less than 0.1 mm in diameter. The fluence distribution for each laser pulse was recorded on Kodak 1-Z spectroscopic emulsion, and the absolute fluence for each shot was computed by the same normalization procedure described for 355 nm beams. Fluence measurements at 248 nm were typically accurate to about 10%.

In experiments at both 248 nm and 355 nm, each site on a sample was irradiated only once. A Nomarski microscope was used to photograph each test site (at magnification of 100-400) before and after it was irradiated. Test sites were also visually inspected with both Nomarski and either bright-field or dark-field microscopy, and with the unaided eye using backlighting with white light. Surface damage was defined to be a permanent alteration of the surface detectable by these inspections. In some tests of window materials, bulk damage occurred at fluences below normal surface damage thresholds. Bulk damage consisted of isolated microfractures which were visible when irradiated with a beam from a He-Ne laser or with intense white light.

Damage thresholds were taken to be the average of the highest fluence that caused no damage and the lowest fluence causing damage. For most samples the boundary between damaging and nondamaging fluences was sharply defined and thresholds could be determined within 10-15% by using only 5-10 shots per sample. In a few of the coatings, defects which damaged at the lowest fluence were separated by a distance comparable to the beam diameter. For these samples, damaging and nondamaging fluences were sometimes intermingled over a fluence range as large as 30% of the threshold fluence.

#### 248 nm damage threshold results

##### Fused silica and UV transmitting borosilicate glass

Rajner et. al.<sup>1</sup> reported threshold measurements for five samples of Suprasil II fused silica, from Heraeus-Amersil, Inc., one sample of 7940 fused silica, from Corning Glass Works, Inc., and one sample of a UV-transmitting glass, UVFK54, from Schott Glass Technologies, Inc. Maximum nondamaging fluences for the fused silica samples were set by the thresholds for rear surface damage, which ranged from 5 to 9 J/cm<sup>2</sup>. Front surface damage thresholds ranged from 8-13 J/cm<sup>2</sup>, and the only incidence of bulk damage was self-focusing tracks induced in the 7940 sample at fluences above the threshold for rear surface damage. Bulk damage was a limiting problem in the UVFK54 in which color centers were induced in single shots at fluences as low as 2 J/cm<sup>2</sup>.

One fused silica sample was repolished with high purity ZrO<sub>2</sub> and another was bowl-feed polished<sup>2</sup> with CeO<sub>2</sub>, but thresholds for these samples were comparable to those of surfaces fabricated by conventional fresh-feed polishing with CeO<sub>2</sub>.

## Fluoride crystals

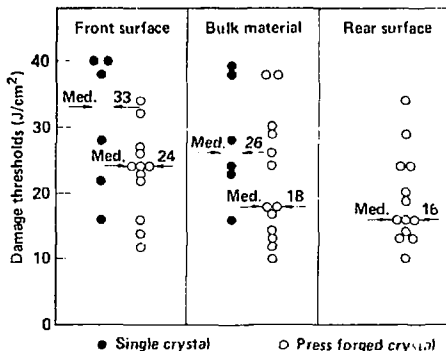
Six single-crystal samples of LiF were tested, as well as 13 fine-grained polycrystalline samples made by press forging. Both types of samples were cut from four different boules to avoid biasing the data to the characteristics of an individual boule. Fig. 2 shows individual and median damage thresholds for these samples. Thresholds for rear-surface damage of the single-crystal samples could not be determined because the surfaces had a high density of polishing scratches.

The damage morphology of both single crystals and forged crystals suggested that the surface absorption of these samples was spatially homogeneous. Damage at fluences slightly above threshold, produced a uniform alteration of the surface, possibly melting and recrystallization. At fluences well above threshold, surface damage in the forged crystals consisted of cracks and pits.

Three CaF<sub>2</sub> crystals were also tested, as well as one sample each of MgF<sub>2</sub>, BaF<sub>2</sub> and NaF. Thresholds for these samples are given in Fig. 3. To allow easy comparison of thresholds of all the fluoride crystals tested, Fig. 3 also shows the median and range of thresholds of the LiF crystals. The threshold surface-damage morphology varied for each sample, but in general consisted of highlighting existing surface defects and polishing scratches. Only for MgF<sub>2</sub> and NaF did the bulk threshold for damage exceed the threshold for front-surface damage. Except for one CaF<sub>2</sub> crystal, which had an unusually low threshold, and the BaF<sub>2</sub> crystal, rear-surface thresholds of these additional fluorides are comparable to those of LiF crystals.

Three of the samples, one each of MgF<sub>2</sub>, BaF<sub>2</sub> and CaF<sub>2</sub>, had been tested earlier using 266 nm pulses with durations of 0.1 and 0.7 ns.<sup>3</sup> Those thresholds and the 20 ns, 248 nm thresholds are shown in Fig. 4 as a function of pulse duration. The slopes of the straight-line fits to these few data points indicate that these front-surface thresholds increase as the square root of the pulsewidth.

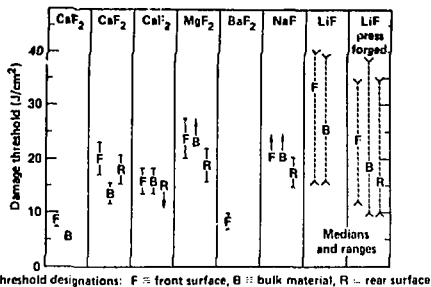
Figure 2. Damage thresholds of six single-crystalline samples of LiF and 13 press-forged LiF samples measured with 248 nm, 20 ns pulses.



## KDP and isomorphs

Threshold measurements were made on four potassium deuterium phosphate (KD\*P) crystals, and one crystal each of KDP and of aluminum dihydrogen phosphate (ADP).<sup>1</sup> These crystals are mechanically soft and difficult to polish, and all surfaces tested had a high density of polishing scratches that could be observed with a Nomarski microscope. Front surface thresholds of these crystals, shown in Fig. 5, ranged generally from 3 to 5 J/cm<sup>2</sup> although the threshold of the KDP sample was greater than 6 J/cm<sup>2</sup>. This result can be compared with the surface threshold of a KDP crystal that was measured earlier with 0.7 ns, 266 nm pulses,  $6.5 \pm 1.4$  J/cm<sup>2</sup>.<sup>3</sup> Since thresholds for 248 nm and 266 nm pulses should be approximately equal, the available data suggest that UV thresholds of KDP are approximately constant over the range of pulse durations from 0.7 ns to 20 ns.

Figure 3. Laser-damage thresholds of fluoride crystals measured with 248 nm 20 ns pulses.



Threshold designations: F = front surface, B = bulk material, R = rear surface

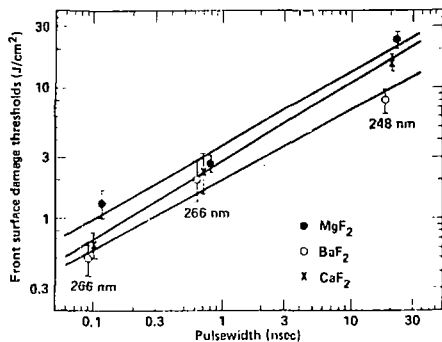


Figure 4. Pulsewidth dependence of front-surface laser-damage thresholds of fluoride crystals in the UV.

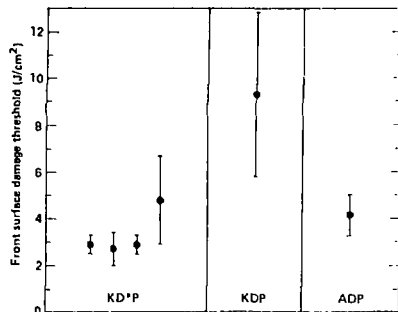


Figure 5. Front-surface laser-damage thresholds of KDP isomorphs measured with 248 nm, 20 ns pulses.

#### Multilayer coatings containing scandium oxide

In a survey conducted by the Naval Weapons Center of coating materials for the XeF laser (353 nm wavelength), high reflectivity coatings of scandium oxide ( $\text{Sc}_2\text{O}_3$ ) and magnesium fluoride ( $\text{MgF}_2$ ) exhibited relatively high damage resistance.<sup>4</sup> Damage thresholds at 248 nm of laser coatings containing  $\text{Sc}_2\text{O}_3$  were subsequently studied in detail by LLNL and OCLI.<sup>5</sup>

The two types of laser coatings studied were high reflectivity (HR) coatings and anti-reflection (AR) coatings. Coating designs and deposition methods which had proven effective for 1 $\mu\text{m}$  laser coatings were used in this study.<sup>6,7</sup> The effects of combining  $\text{Sc}_2\text{O}_3$  with both silica ( $\text{SiO}_2$ ) and  $\text{MgF}_2$  were investigated. The studies of HR coatings included the effects of overcoat layers, substrate materials, deposition temperature, and number of layers in the coatings. For AR coatings, the effects of undercoat layers and choice of low index material were tested. A large number of coatings were tested to determine the reproducibility of results. With optimum coating designs and deposition conditions, the damage thresholds of both HR and AR coatings were consistently above 6  $\text{J}/\text{cm}^2$  for 248 nm, 20 ns pulses.

**High reflectivity coatings.** The HR coating design consisted of 19 quarterwave-thick layers of  $\text{Sc}_2\text{O}_3/\text{MgF}_2$ , although some 31 layer designs were also tested. All coatings were deposited by electron beam evaporation. Each of the coatings was deposited on both conventionally polished fused silica and BK-7 glass substrates at substrate temperatures of 150 C and 250 C. To test the effect of overcoat layers, halfwave-thick overcoats of either  $\text{MgF}_2$  or  $\text{SiO}_2$  were added to the top of the quarterwave stacks of some samples. These overcoat layers did not change the reflectivity or the electric field distribution in the HR stack, but have been shown to increase damage thresholds for HR coatings.<sup>6</sup>

A total of 45 HR coatings were tested as part of this study: 15 without overcoat, 15 with  $\text{MgF}_2$  overcoat, and 15 with  $\text{SiO}_2$  overcoat. The coatings were deposited in five separate runs of nine samples each. In each run, the basic 19 layer (or 31 layer) coating was deposited simultaneously on all nine substrates. Then six substrates were covered with masks and the halfwave  $\text{MgF}_2$  overcoat was added to three of the substrates. These three were then covered and the  $\text{SiO}_2$  overcoat was added to three of the remaining six samples. Thus, the only difference between the coatings in each run was the overcoat.

Figs. 6 and 7 show the dependence of the measured damage thresholds of HR coatings on substrate material, deposition temperature, and type of overcoat layer. Overcoat layers had the most pronounced effect on damage thresholds. All films without an overcoat had thresholds below 4  $\text{J}/\text{cm}^2$ , while all with an overcoat had thresholds above 4  $\text{J}/\text{cm}^2$ . The median thresholds for nonovercoated and overcoated films were 3.1  $\text{J}/\text{cm}^2$  and 6.3  $\text{J}/\text{cm}^2$ , respectively. Among overcoated films, the median threshold for coatings with  $\text{MgF}_2$  overcoats was 20% greater than the median threshold for  $\text{SiO}_2$  overcoats.

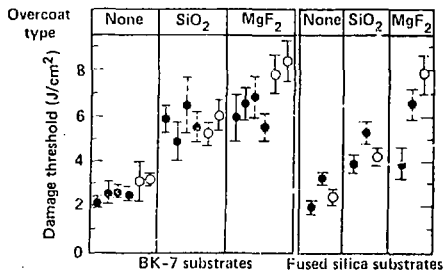


Figure 6. 248 nm, 20 ns laser-damage thresholds of  $\text{Sc}_2\text{O}_3/\text{MgF}_2$  HR coatings deposited at 150°C. Solid circles are data from 19-layer coatings and open circles represent 31-layer coatings. Dashed error bars signify samples from a repeat coating run.

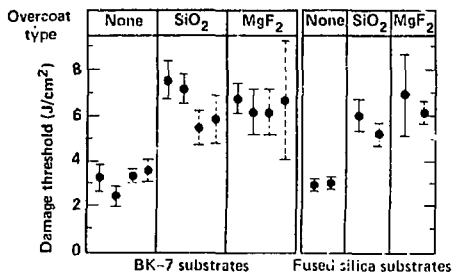


Figure 7. 248 nm, 20 ns laser-damage thresholds of 19-layer  $\text{Sc}_2\text{O}_3/\text{MgF}_2$  HR coatings deposited at 250°C. Dashed error bars signify samples from a repeat coating run.

**Antireflection coatings.** A total of twenty-four AR coatings were tested as part of this study: twelve each of two material combinations  $\text{Sc}_2\text{O}_3/\text{MgF}_2$  and  $\text{Sc}_2\text{O}_3/\text{SiO}_2$ . The coatings were made in four separate runs of six parts each. Coatings were deposited on bowl-feed polished fused silica at a substrate temperature of 150 C. The effect of an undercoat layer on damage resistance was also tested. A halfwave-thick layer of either  $\text{MgF}_2$  or  $\text{SiO}_2$  was deposited between the AR coating and the substrate of some of the samples. This layer did not affect the electric field distribution either in the four-layer AR coating or at the substrate interface, but has been shown to be effective in increasing damage thresholds in earlier work.<sup>6</sup> Movable masks in the coating chamber allowed the undercoat layers to be deposited on their respective parts and then the AR coating to be deposited simultaneously on all the parts.

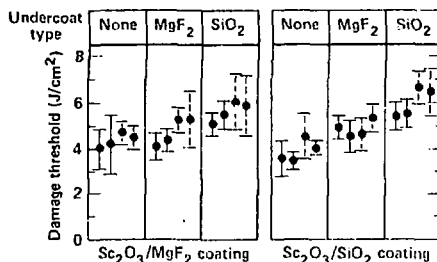
The reflectivities of  $\text{Sc}_2\text{O}_3/\text{MgF}_2$  AR coatings were below 0.1% at 248 nm. Those of  $\text{Sc}_2\text{O}_3/\text{SiO}_2$  films were between 0.15 and 0.2%. Even though the AR coatings were deposited on fused silica substrates, they did not exhibit the crazing observed in HR films on fused silica.

Damage thresholds of the AR coatings are shown in Fig. 8. The only variable which significantly increased damage thresholds was the presence or absence of undercoats. Averaged over all coatings made in four runs, improvements with SiO<sub>2</sub> and MgF<sub>2</sub> undercoats were 38% and 17% respectively.

There was no significant difference between damage thresholds of Sc<sub>2</sub>O<sub>3</sub>/MgF<sub>2</sub> and Sc<sub>2</sub>O<sub>3</sub>/SiO<sub>2</sub> coatings. The Sc<sub>2</sub>O<sub>3</sub>/SiO<sub>2</sub> films had a wider range of thresholds, and those with SiO<sub>2</sub> undercoats had the highest median threshold (6.1 J/cm<sup>2</sup>) of all the AR coatings and undercoat combinations tested.

Reproducibility of AR coating thresholds was also good. In each run six coatings were deposited, two each of three designs. For the pairs of identical coatings made in each run, thresholds varied, on the average, by only 6%. Each deposition was repeated, providing a total of four coatings of each design. The average variation in thresholds among these sets of four coatings was 12%.

Figure 8. 248 nm 20 ns laser-damage thresholds of AR coatings. Dashed error bars signify samples from a repeat coating run



#### UV coating materials survey

Lengthy studies of a few materials, as described in the preceding section, allow optimization of the deposition parameters for these materials, and provide an adequate data base to evaluate the coatings. However, time and expense limits the number of such studies that can be performed. The following materials survey was conducted with the goal to identify materials with best performance. In particular, we were interested to see if relationships existed between damage thresholds of coatings and other physical or optical properties which could guide the selection of optimum materials.

Both single layer coatings and multilayer high reflectivity coatings were tested.<sup>8</sup> Single layers are easily deposited, so many materials can be quickly prepared. The damage thresholds of single layer films may, however, be affected by the substrate. Damage thresholds of HR coatings are not affected by the substrate.

All coatings were deposited by electron-beam evaporation of the materials onto fused silica substrates that had been bowl-feed polished at OCLI. For single layer films, the refractive index, absorption, stress, environmental stability and the position of the UV handedge were measured at OCLI. Index of refraction for the individual coating materials was calculated from the measured reflectance and transmittance of thick, single-layer films. The absorption coefficient of a film material was measured by coating a halfwave thick layer of the material on a high reflector and measuring the decrease in reflectance. Film stress was determined by interferometric measurement of the stress-induced flexure of coated substrates 0.38 mm in thickness. The absorption edge was defined to be the wavelength at which the transmission of a coating with a 1.5 μm optical thickness was 50%. Since transmission measurements could not be made at wavelengths below 200 nm, the hand edge could not be measured in some films. The films were subjected to an environmental evaluation consisting of standard abrasion and adhesion tests and 24 hours of exposure to high humidity.

Physical and optical properties measured for the halfwave-thick films are given in Table 1. The attenuation coefficient  $k$  (imaginary part of the complex index of refraction  $n+ik$ ) was generally small in the fluorides, except for Nb<sub>3</sub>AlF<sub>6</sub> and NaF, and large in the oxides, except in Al<sub>2</sub>O<sub>3</sub> and SiO<sub>2</sub>, which have absorption edges below 200 nm. Two



oxide materials, MgO and Al<sub>2</sub>O<sub>3</sub>, failed the environmental test. While it has traditionally been difficult to control deposition of MgO, failure of Al<sub>2</sub>O<sub>3</sub> is unusual.

**Single layer films.** Halfwave thick layers of 15 oxide and fluoride films were deposited. Most of the coatings had good cosmetic appearance and contained only isolated defects with typical dimensions of 1  $\mu$ m. There were however some exceptions. Films of YF<sub>3</sub> crazed, presumably due to high stress. Some areas on Na<sub>3</sub>AlF<sub>6</sub> films were clear, but other areas had a streaked appearance. Films of both ZrO<sub>2</sub> and NaF were hazy. This appearance is atypical of ZrO<sub>2</sub>.

The damage thresholds measured for two samples of each material are given in Fig. 9. Thresholds ranged from less than 1 J/cm<sup>2</sup> in ZrO<sub>2</sub>, which is comparable to the damage fluence for some metallic films, to 25 J/cm<sup>2</sup> in ThF<sub>4</sub>, which is about twice the front-surface threshold of bare, polished fused silica.<sup>1</sup> This result is unusual because thresholds of coated surfaces rarely exceed those of bare surfaces.

Table 1. Physical and Optical Properties of Single-Layer Films with Optical Thickness of 124 nm

Material	Refractive Index (n) at 248 nm	Attenuation Coefficient (k) at 248 nm	Absorption Band <sup>1</sup> Edge, nm	Stress <sup>2</sup> KPSI	Environmental Stability
ZrO <sub>2</sub>	2.25	.006	230	-39 <sup>1</sup>	Pass
Na <sub>3</sub> AlF <sub>6</sub>	1.35	.007	S	-4	Fail
ThO <sub>2</sub>	1.90	.005	200	-72	Pass
Y <sub>2</sub> O <sub>3</sub>	2.10	.002	210	+11	Pass
HfO <sub>2</sub>	2.25	.002	215	-59	Pass
Sc <sub>2</sub> O <sub>3</sub>	2.11	.002	205	-23	Pass
MgO	1.83	.007	200	-5	Fail
Al <sub>2</sub> O <sub>3</sub>	1.72	< .001	< 200	-86	Fail
YF <sub>3</sub>	1.54	< .001	< 200	-49	Pass
NaF	1.35	.009	S	-8	Fail
LiF	1.37	.001	<< 200	-1	Marginal
MgF <sub>2</sub>	1.43	< .001	< 200	-50	Pass
LaF <sub>3</sub>	1.59	.001	< 200	-91	Pass
SiO <sub>2</sub>	1.44	.001	< 200	+4	Pass
ThF <sub>4</sub>	1.59	< .001	<< 200	-30	Pass

1. Absorption edge is 50% point in transmission; 200 means some absorption at 200 nm; << 200 means no absorption at 200 nm; S means absorption edge probably masked by scattering.

2. +, compressive; -, tensile.

Figure 10 shows the film thresholds versus physical and optical properties of the films. Thresholds were largest in the films with low refractive index, which (excepting SiO<sub>2</sub>) were all fluorides. Thresholds were also largest in films with low absorption, which were generally the low index films with bandedges below 200 nm. In fact, the correlation between absorption and thresholds was sufficiently strong to suggest that the apparent correlation between threshold and index is accidental. NaF was an exception, being very absorptive, but having a moderately large threshold and scatter. No correlation was observed between stress and damage threshold.

Our results are generally similar to those of Newnam and Gill<sup>9</sup> who used 22 ns, 266 nm pulses to test single layers of six oxide materials and three fluoride materials, and those of Walker, et al.,<sup>10</sup> who tested films of six oxides and three fluorides with 15 ns, 266 nm pulses. Among these three studies, both the ordering and actual threshold values vary considerably, confirming that it is difficult to establish true comparisons of materials in thin-film form. The general correlation between high thresholds and low refractive indices is present in all three studies. This correlation was first observed by Turner,<sup>11</sup> and later developed into the form of a scaling law by Bettis, et al.<sup>12</sup>

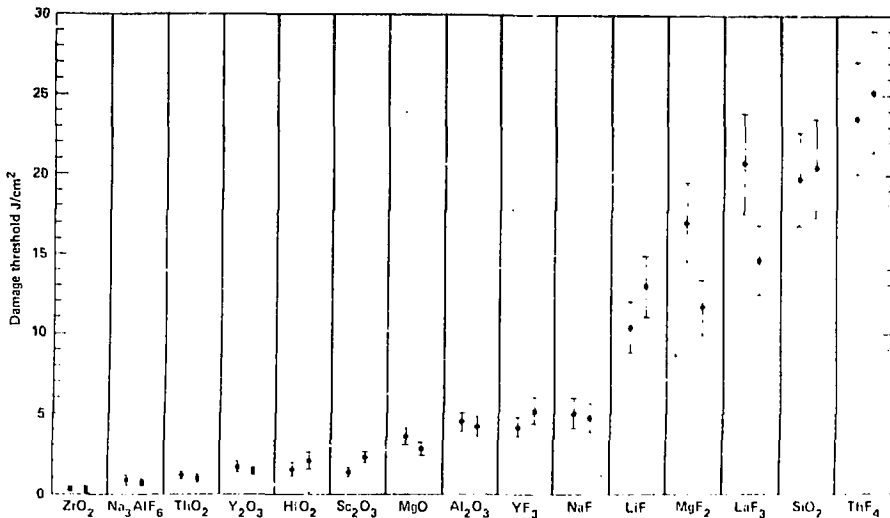


Figure 9. Laser-damage thresholds of halfwave-thick films measured with 248 nm, 20 ns pulses.

The scaling law predicts some of the results of the three UV damage studies. However, it is based on the premise that thresholds should scale according to the strength of the local electric field, and would not be applicable if linear absorption were the dominant mechanism for damage.

Although the material characteristic responsible for damage in a given material is not known, trends in the entire set of data identify the characteristics that are associated with good resistance to damage by 248 nm irradiation. The film material should have low refractive index, low absorption, bandedge located at a wavelength well below 248 nm, good cosmetic appearance, and good environmental stability when exposed to high humidity. For single layer films, stress did not influence thresholds, but this does not necessarily imply that film stress will be unimportant in multilayer coatings.

**High reflectivity coatings.** HR coatings of 13 high index/low index combinations were deposited. Four coatings of each material combination were made, two in each of two coating runs. Each coating had a minimum of 15 quarterwave-thick layers and was overcoated with a halfwave-thick layer of the low index material used in the reflector stack. The coatings were deposited on conventionally-polished substrates of BK-7 glass.

Damage thresholds of these HR coatings are shown in Fig. 11. Coatings with the lowest thresholds contained the high index materials ZrO<sub>2</sub> and ThO<sub>2</sub>, which had the lowest thresholds as single layers. In contrast, the low index material Na<sub>3</sub>AlF<sub>6</sub> had a low threshold as a single layer, but when combined with Al<sub>2</sub>O<sub>3</sub>, produced a reflector with moderate threshold. Reflectors of Sc<sub>2</sub>O<sub>3</sub>/MgF<sub>2</sub> and MgO/LiF had the highest thresholds, the median values being, respectively, 5.6 and 7.0 J/cm<sup>2</sup>. An interesting, but not understood, fact is that the highest HR coating thresholds were considerably higher than the thresholds of single layers of the high index materials, and considerably less than thresholds of single layers of the low index materials.

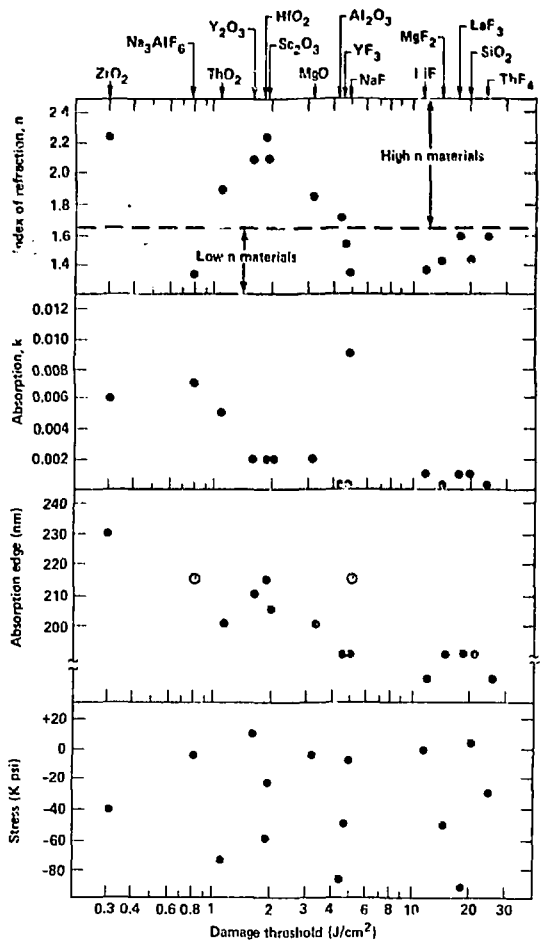


Figure 10. Index of refraction, absorption, position of the UV band edge and film stress for 15 UV coating materials plotted as a function of the average of the damage thresholds measured on two halfwave-thick samples of each material.

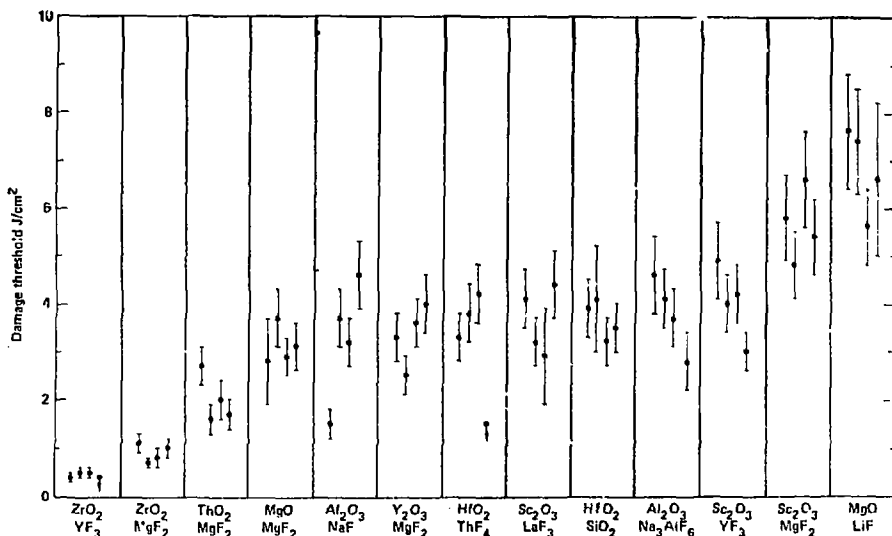


Figure 11. Laser damage thresholds (20 ns, 248 nm) of quarterwave-stack multilayer highly reflecting coatings made from 13 combinations of high-index and low-index materials.

### 355 nm damage threshold results

#### Fused silica and KDP crystals

Damage thresholds of fused silica and KDP crystals were measured by Staggs and Rainer.<sup>13</sup> Fused silica is the only glass so far demonstrated to be capable of transmitting 355 nm beams at intensities of 2-5 GW/cm<sup>2</sup> without exhibiting nonlinear absorption or being discolored by solarization.<sup>14</sup> The samples of fused silica tested were made of three types of highly pure flame-fusion silica, and two materials made from naturally occurring quartz. These materials are listed in Table 2. Surfaces were polished by several vendors with commercially available cerium oxide abrasives.

Table 2. Types of Silica Tested

Material Designation	Material Type	Vendor
7940	flame fusion	Corning Glass Works, Inc.
Optosil I	fused natural quartz	Heraeus-Amersil, Inc.
Suprasil II	flame fusion	Heraeus-Amersil, Inc.
ES	flame fusion	Nippon Silica Glass Co., Ltd.
DX	fused natural quartz	Nippon Silica Glass Co., Ltd.

Surface damage thresholds for 22 samples tested, given in Fig. 12, ranged from 1-14 J/cm<sup>2</sup>, but there was no obvious relationship between thresholds and the type of silica. Instead, thresholds at 355 nm seemed to depend solely on the polishing history. To illustrate this point, Fig. 13 is a histogram of thresholds measured on 12 samples including four types of silica polished by one vendor. The thresholds are closely grouped with a median of almost 10 J/cm<sup>2</sup>. Further, when these surfaces were etched with HF acid, the etched surface was essentially featureless. By contrast, etching samples with low thresholds revealed significant subsurface structure. Therefore, it is likely that low thresholds on some surfaces resulted from incorporation of polishing material into the surface.

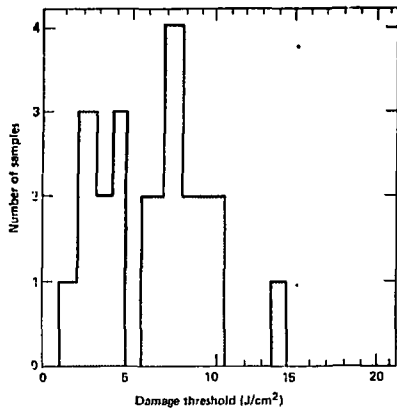


Figure 12. Front-surface damage thresholds measured with 355 nm, 0.6 ns pulses on fused silica samples polished by several vendors.

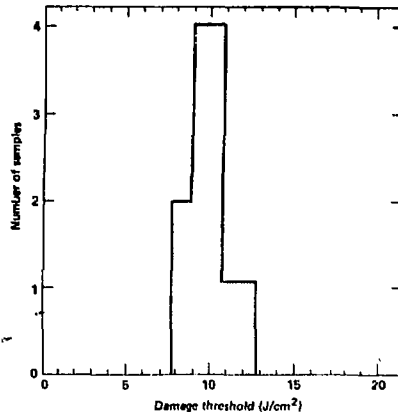


Figure 13. Front-surface damage thresholds measured with 355 nm, 0.6 ns on 12 fused silica samples polished by one vendor.

The measurements of bulk damage thresholds in KDP crystals were made with a weakly convergent beam whose intensity did not vary significantly along the 2 cm path length through the crystal. Bulk damage can be observed in such experiments only when the threshold for bulk damage is less than the front surface damage threshold, which is generally true for KDP.<sup>15</sup> The bulk damage produced in KDP by 355 nm beams consisted of isolated microfractures, whose volume density depended on the quality of the crystal and the fluence. In the best crystals, at fluences near threshold, only one or two microfractures were created. In some crystals with low thresholds, there were hundreds of microfractures per cubic centimeter in a trail filling the entire beam path.

Damage thresholds measured in 1-on-1 and n-on-1 tests<sup>15</sup> of KDP crystals are given in Fig. 14. The crystals were samples taken from large boules grown to provide large aperture crystals for harmonic converters on NOVA. The median 1-on-1 and n-on-1 thresholds of these crystals were, respectively, 2.3 and 4.2 J/cm<sup>2</sup>. Therefore, repetitive subthreshold irradiation of test volumes with 355 nm pulses produced an average increase in damage thresholds.

#### High reflectivity coatings

Multilayer HR coatings of various materials were tested, as well as the effects of overcoat layers and the use of nonquarterwave layers to suppress the standing wave electric fields in either the high or low index material.<sup>16</sup>

The first set of coatings tested the commonly used high refractive index materials ZrO<sub>2</sub>, Ta<sub>2</sub>O<sub>5</sub> and HfO<sub>2</sub> which are transparent at 355 nm. The low index material for all coatings was SiO<sub>2</sub>. All coatings were composed of 15 quarterwave thick layers centered at 355 nm. Eight coatings of each material combination were prepared and tested; four had a halfwave thick overcoat of SiO<sub>2</sub> and the other four had no overcoat. To test reproducibility of coatings from run to run, two coatings of each type were prepared in each of two coating runs.

The damage threshold measurements are shown in Fig. 15. The median threshold in J/cm<sup>2</sup> for (overcoated/nonovercoated) samples are: (2.4/3.0) for ZrO<sub>2</sub>/SiO<sub>2</sub>, (1.9/2.5) for Ta<sub>2</sub>O<sub>5</sub>/SiO<sub>2</sub> and (1.1/1.1) for HfO<sub>2</sub>/SiO<sub>2</sub>. In all cases, the samples without overcoats had thresholds which were equal to or greater than the companion overcoated sample. This result is counter to previous experience with HR coatings for 1064 nm and 248 nm wavelength.

Figure 14. Bulk damage thresholds (0.6-ns, 355-nm pulses) of KDP samples from large boules. For the 1-on-1 tests samples were irradiated once at each site; for n-on-1 tests samples were irradiated at a particular site with sequentially higher fluences until damage occurred.

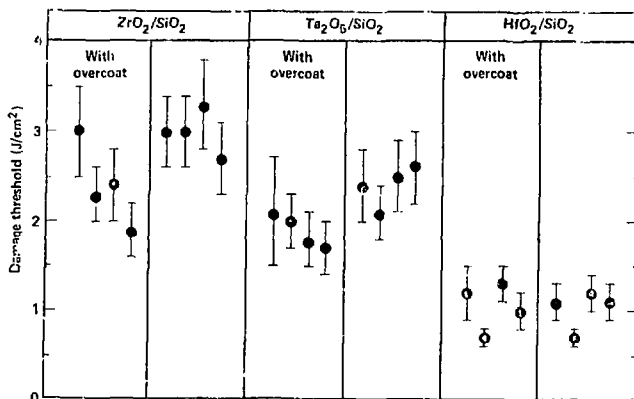
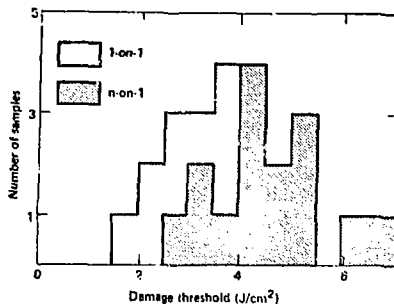


Figure 15. Laser damage thresholds measured with 355 nm, 0.6 ns pulses in HR coatings made from three combinations of materials. The overcoats were halfwave-thick layers of SiO<sub>2</sub>.

Coatings of Sc<sub>2</sub>O<sub>3</sub>/MgF<sub>2</sub>, which had been found to have high damage thresholds for 248 nm pulses, were also tested at 355 nm. A total of 24 coatings were prepared, each consisting of 25 quarterwave-thick layers. Coatings were deposited in two coating runs; one with substrate temperature of 150 C and the other at 250 C. In each run, four coatings received no overcoat, four received a halfwave overcoat of SiO<sub>2</sub> and four a halfwave overcoat of MgF<sub>2</sub>. All coatings had excellent cosmetic appearance with no visible defects and reflectance greater than 99.5% at 355 nm.

The damage threshold results for these coatings are summarized in Fig. 16. Damage thresholds were not improved by the addition of overcoat layers and thresholds of the coatings deposited at 250 C were higher than for those deposited at 150 C. Both results agree with tests of other coating materials at 355 nm and disagree with results from studies of coatings for 248 nm or 1064 nm.

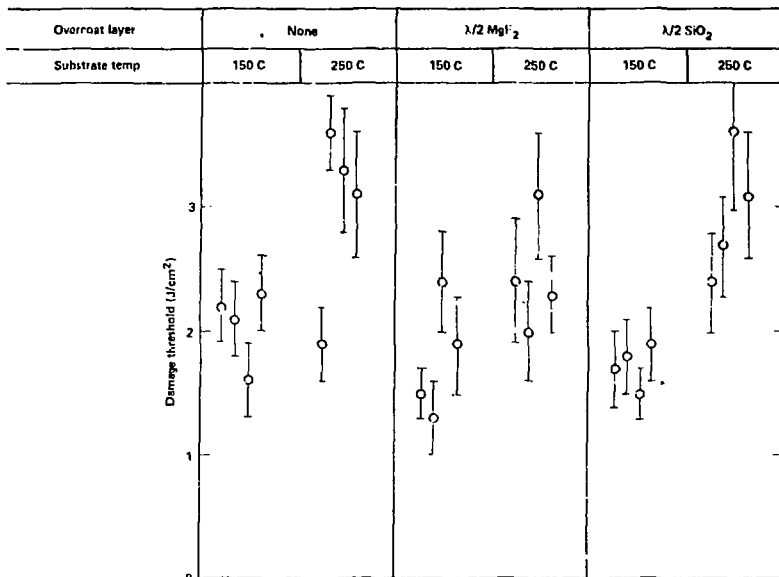


Figure 16. Laser-damage thresholds measured with 355 nm, 0.6 ns pulses on Sc<sub>2</sub>O<sub>3</sub>/MgF<sub>2</sub> HR coatings deposited on BK-7 glass substrates held at either 150°C or 250°C. Some of the HR coatings had halfwave-thick overcoats of either MgF<sub>2</sub> or SiO<sub>2</sub>.

Subsequently, 24 HR coatings were prepared consisting of 10 alternating layers of Sc<sub>2</sub>O<sub>3</sub> and SiO<sub>2</sub> followed by 11 alternating layers of Sc<sub>2</sub>O<sub>3</sub> and MgF<sub>2</sub> and a halfwave-thick MgF<sub>2</sub> overcoat. Some of these coatings had nonquarterwave outer layers with thicknesses chosen to suppress the internal standing wave intensity in either the high index or low index layers. Use of nonquarterwave layers in AR coatings was initiated by DeBell,<sup>17</sup> and subsequently discussed by Newnam<sup>18</sup> and Apfel<sup>19</sup>.

Measured thresholds for these 24 coatings, shown in Fig. 17, varied systematically as anticipated from the alterations made in the thickness of the outer coating layers. The median threshold for standard Sc<sub>2</sub>O<sub>3</sub>/MgF<sub>2</sub> quarterwave stacks was 3.6 J/cm<sup>2</sup>, which is slightly higher than those measured on HR coatings made using ZrO<sub>2</sub>, HfO<sub>2</sub> or Ta<sub>2</sub>O<sub>5</sub>. Reducing the thickness of one low index layer in the Sc<sub>2</sub>O<sub>3</sub>/MgF<sub>2</sub> coating increased the field in the Sc<sub>2</sub>O<sub>3</sub> and reduced the threshold. Reducing the intensity in one or two outer, high index layers increased thresholds. The median threshold of 5.1 J/cm<sup>2</sup> for coatings with two modified layers is the highest threshold for an HR coating observed thus far for 0.6 ns, 355 nm pulses.

The last material combinations evaluated for HR coatings were SmF<sub>3</sub>/MgF<sub>2</sub> and SmF<sub>3</sub>/SiO<sub>2</sub>. Films of SmF<sub>3</sub> are highly stressed and crazing frequently occurs in HR coatings made with either SmF<sub>3</sub>/SiO<sub>2</sub> or SmF<sub>3</sub>/MgF<sub>2</sub>. Therefore, a basic reflector was fabricated of ZrO<sub>2</sub>/SiO<sub>2</sub>, and SmF<sub>3</sub> was used to replace the ZrO<sub>2</sub> in the outer layers, which are the only layers that are intensely irradiated. OCLI provided 12 coatings, each of which contained 15 alternating layers of ZrO<sub>2</sub> and SiO<sub>2</sub>. One or two pairs of either SmF<sub>3</sub>/SiO<sub>2</sub> or of SmF<sub>3</sub>/MgF<sub>2</sub> were added and all of the coatings received a halfwave thick overcoat of SiO<sub>2</sub>. Thresholds for these coatings, given in Fig. 18, were comparable to those measured for HR coatings made of either ZrO<sub>2</sub>/SiO<sub>2</sub> or of Ta<sub>2</sub>O<sub>5</sub>/SiO<sub>2</sub>. Overcoats were ineffective in improving thresholds.

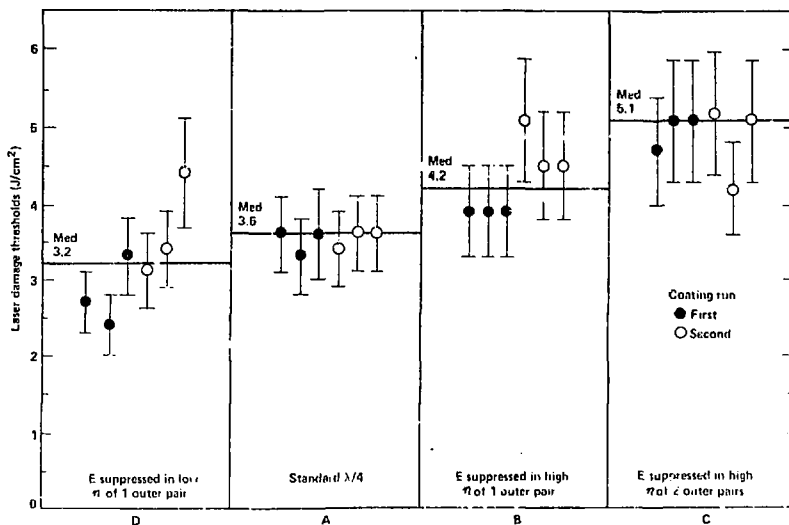


Figure 17. Laser damage thresholds measured with 355 nm, 0.6 ns pulses in  $\text{Sc}_2\text{O}_3/\text{SiO}_2/\text{MgF}_2$  HR coatings with outer layers altered to increase the standing wave intensity in either the high-index material ( $\text{Sc}_2\text{O}_3$ ), design D, or the low-index material ( $\text{MgF}_2$ ), designs B and C.

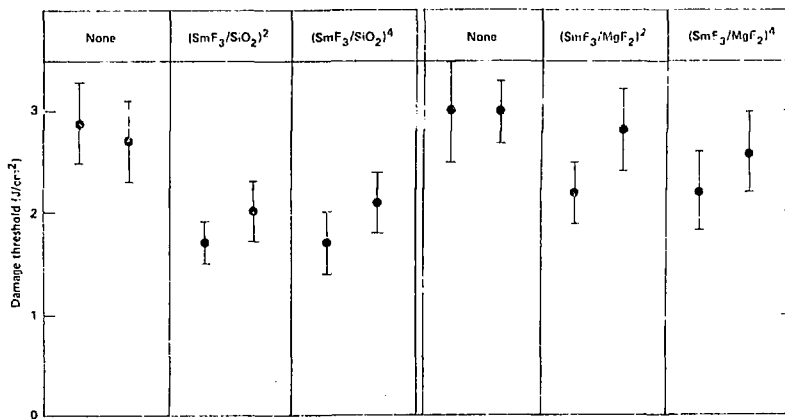


Figure 18. Laser damage thresholds measured with 355 nm, 0.6 ns pulses on  $\text{ZrO}_2/\text{SiO}_2$  HR coatings with either 0, 2 or 4 added pairs of either  $\text{SmF}_3/\text{SiO}_2$  or  $\text{SmF}_3/\text{MgF}_2$ .



### Antireflection coatings

Fifteen different AR coatings of two basic types were studied by Hart *et al.*<sup>20</sup> Coatings of the first type were conventional four-layer, non-quarterwave designs with alternating layers of materials with high refractive index and low refractive index. Coatings of the second type were composed of two different low index materials using three- to six-layer quarterwave designs. The high index materials ( $\text{Sc}_2\text{O}_3$ ,  $\text{ZrO}_2$ , and  $\text{HfO}_2$ ) were chosen because they are UV transparent and commonly used in the industry. The low index materials ( $\text{LiF}$ ,  $\text{MgF}_2$ ,  $\text{SiO}_2$ ,  $\text{ThF}_4$ ,  $\text{LaF}_3$ , and  $\text{SmF}_3$ ) were chosen because they had high damage thresholds when tested as single layers at 248 nm as described above.

All coatings were deposited by electron beam evaporation on bowl-iced polished Suprasil II fused silica substrates. Only bowl-iced polished substrates were used for this study because coatings on this type of substrate historically have higher damage thresholds than similar coatings on conventionally-polished substrates.<sup>21</sup>

The results of the laser damage threshold measurements are summarized in Figs. 19 and 20 and in Table 3. As seen in Fig. 19, the average damage thresholds for the high index coatings were essentially the same (2.4 - 2.6  $\text{J}/\text{cm}^2$ ), except for the  $\text{Sc}_2\text{O}_3/\text{MgF}_2$  coatings, which had an average threshold of 3.1  $\text{J}/\text{cm}^2$ , and one coating had a threshold of 3.5  $\text{J}/\text{cm}^2$ .

Table 3. Table of Laser Damage Thresholds of AR Coatings for 355 nm, 0.6 ns Pulses

Material Combination	Coating Type <sup>†</sup>	Average Threshold ( $\text{J}/\text{cm}^2$ )
$\text{Sc}_2\text{O}_3/\text{MgF}_2$	High index	3.1
$\text{SmF}_3/\text{MgF}_2$	Low index	2.8
$\text{SmF}_3/\text{SiO}_2$	Low index	2.7
$\text{SiO}_2/\text{MgF}_2$	Low index	2.7
$\text{HfO}_2/\text{SiO}_2$	High index	2.6
$\text{ZrO}_2/\text{SiO}_2$	High index	2.4
$\text{Sc}_2\text{O}_3/\text{SiO}_2$	High index	2.3
$\text{ThF}_4/\text{LiF}$	Low index	2.3
$\text{ThF}_4/\text{SiO}_2$	Low index	2.3
$\text{LaF}_3/\text{SiO}_2$	Low index	2.1
$\text{ThF}_4/\text{MgF}_2$	Low index	2.0
$\text{SiO}_2/\text{LiF} + \text{O/C}$	Low index	1.9
$\text{LaF}_3/\text{MgF}_2$	Low index	1.0

<sup>†</sup>See description of high and low index coatings in the text.

As seen in Fig. 20, the average damage thresholds for the low index coatings (with the exception of  $\text{LaF}_3/\text{MgF}_2$ ) were distributed over the range 1.9 - 2.8  $\text{J}/\text{cm}^2$ . Coatings of  $\text{SmF}_3/\text{MgF}_2$  had the highest average thresholds (2.8  $\text{J}/\text{cm}^2$ ). The highest damage threshold was 3.4  $\text{J}/\text{cm}^2$  for a  $\text{SmF}_3/\text{SiO}_2$  coating. The addition of a halfwave  $\text{SiO}_2$  overcoat to the  $\text{SiO}_2/\text{LiF}$  did not increase its damage threshold to any significant degree.

### Pulsedwidth scaling of damage thresholds

The dependence of damage thresholds at 355 nm on the laser pulse duration was studied by Rainer *et al.*<sup>22</sup> Pulses with durations of 1, 5 and 9 ns were used to test an assortment of AR and HR coatings that had been previously tested with 0.6 ns, 355 nm pulses. The pulses were sliced from longer pulses by a Pockels cell shutter, so prior to amplification they had identical rise and fall times. After being amplified and harmonically converted, the 1 ns pulses had nearly Gaussian waveforms. The longer pulses

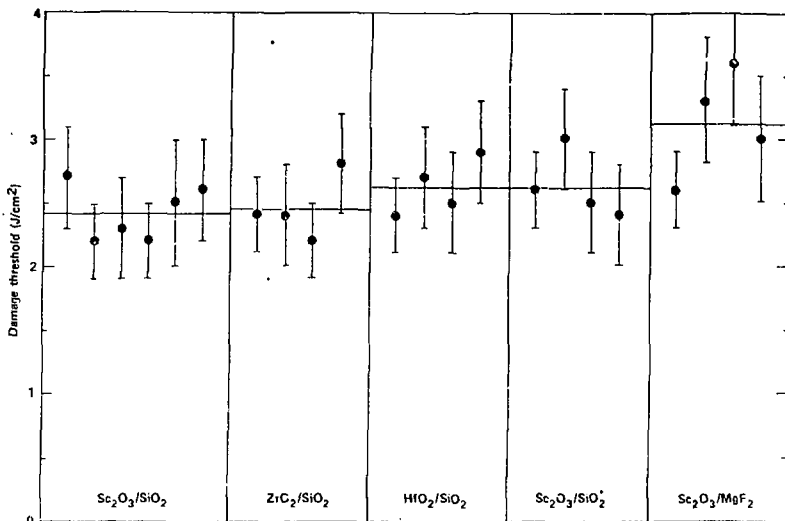


Figure 19. Laser-damage thresholds measured with 355 ns 0.6 ns pulses on AR coatings that contain both low and high index materials. (\*)Dual wavelength 248 nm, 355 nm coatings.

were approximately rectangular, but distorted by gain saturation in laser amplifiers and the nonlinear process of harmonic conversion. At the highest fluences used in these measurements, intensity at the trailing edge of the pulse was about one-half as large as that at the leading edge.

Thresholds measured as a function of pulse duration are shown in Fig. 21. Circled numbers in Fig. 21 identify the sample associated with each set of data. The samples are described in Table 4. The data in Fig. 21 were fitted to a simple power law which assumed that threshold  $T$  varied with pulse duration  $t$  according to  $T=kt^m$ . For five high reflectors,  $m$  ranged from 0.10 to 0.51 and averaged 0.32. For four antireflective coatings,  $m$  ranged from 0.19 to 0.35 and averaged 0.27.

Table 4. Pulsewidth Scaling of Laser Damage at 351-355 nm

#	Coating	Materials	Layers	OC/UC <sup>a</sup>	m <sup>b</sup>
1	HR	Sc <sub>2</sub> O <sub>3</sub> /MgF <sub>2</sub> /SiO <sub>2</sub>	21 <sup>c</sup>	λ/2 MgF <sub>2</sub>	0.37
2	"	ZrO <sub>2</sub> /SiO <sub>2</sub>	15	λ/2 SiO <sub>2</sub>	0.51
3	"	ZrO <sub>2</sub> /SiO <sub>2</sub>	"	None	0.10
4	"	Ta <sub>2</sub> O <sub>5</sub> /SiO <sub>2</sub>	"	"	0.17
5	"	HfO <sub>2</sub> /SiO <sub>2</sub>	"	"	0.46
6	AR	HfO <sub>2</sub> /SiO <sub>2</sub>	4 <sup>c</sup>	λ/2 SiO <sub>2</sub>	0.35
7	"	ZrO <sub>2</sub> /SiO <sub>2</sub>	" <sup>c</sup>	"	0.30
8	"	MgF <sub>2</sub> /SiO <sub>2</sub>	5 <sup>c</sup>	"	0.22
9	"	Sc <sub>2</sub> O <sub>3</sub> /SiO <sub>2</sub>	4 <sup>c</sup>	λ SiO <sub>2</sub>	0.19

- a. OC ≡ overcoat on HR's; UC ≡ undercoat on AR's.  
 b. Temporal scaling coefficient: threshold =  $kt^m$ .  
 c. Nonquarterwave-thick layers.

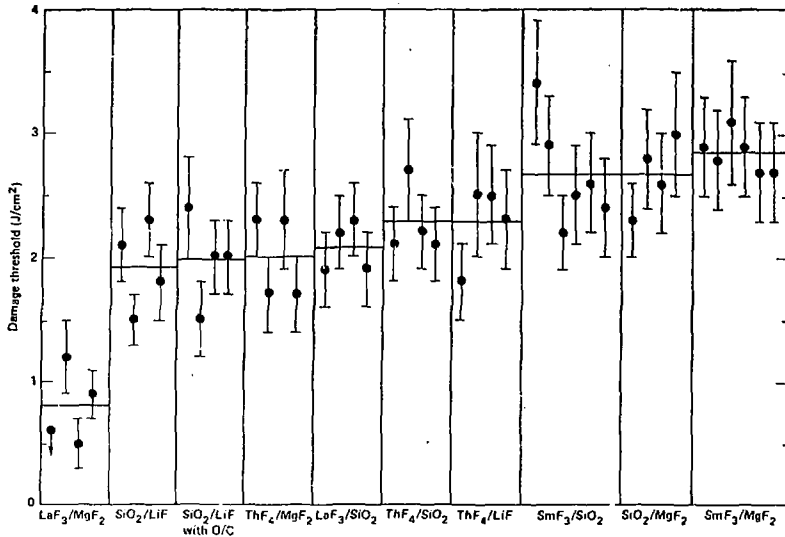


Figure 20. Laser-damage thresholds measured with 355 nm, 0.6 ns pulses on AR coatings containing only materials with low or moderate refractive indices.

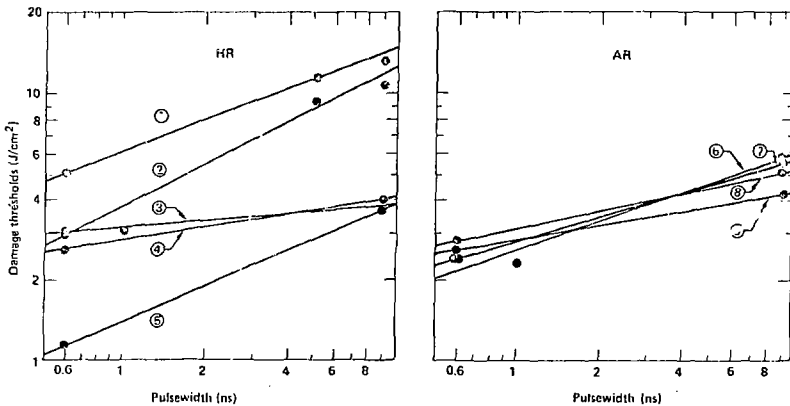


Figure 21. 355 nm laser-damage thresholds of HR and AR coatings as a function of laser pulse duration. Lines are curves fit to the data. Numerals identify samples listed in Table 4.

Values of  $m$  measured in other 355 nm damage experiments span the range  $-0.05 < m < 0.74$ , although most are between 0.3 and 0.4.<sup>23,24,25</sup> These earlier tests were primarily for single layer coatings, but the results are in general agreement with the results obtained in tests of multilayer coatings. However, the range of observed scaling factors is so large that the data provide little insight into the mechanism responsible for damage, and conversely, there is no readily apparent scaling rule that can be used to extrapolate thresholds.

Damage threshold dependence on film layer thickness

An experiment was performed to study the relationship between layer thickness in 355 nm four layer Sc<sub>2</sub>O<sub>3</sub>/SiO<sub>2</sub> AR coatings and thresholds of the coatings.<sup>22</sup> Some layers in conventional 355 nm AR coatings are less than 40 nm in thickness, and it was thought possible that such thin layers might be mechanically weak. Secondly, the experiment provided an excellent evaluation of a recent theory which suggests that thresholds should increase as layer thickness decreases.<sup>26</sup>

All of the coatings contained two Sc<sub>2</sub>O<sub>3</sub> layers and two SiO<sub>2</sub> layers. In a given design, the thickness was different for each of the four layers. Among the four designs, optical thickness  $T$  for all layers in a given design satisfied the following conditions: A.  $T \geq \lambda$ , B.  $\lambda \geq T \geq \lambda/4$ , C.  $T \sim \lambda/4$ , and D.  $T < \lambda/4$ , where  $\lambda$  is 355 nm. Each coating was deposited over a silica undercoat layer which was a fullwave in optical thickness for design A and a halfwave in optical thickness for designs B, C and D.

The coatings were deposited by electron beam evaporation on fused silica substrates that had been bowl-feed polished at OCLT. Two coating runs were made for each design, and three substrates were coated in each run.

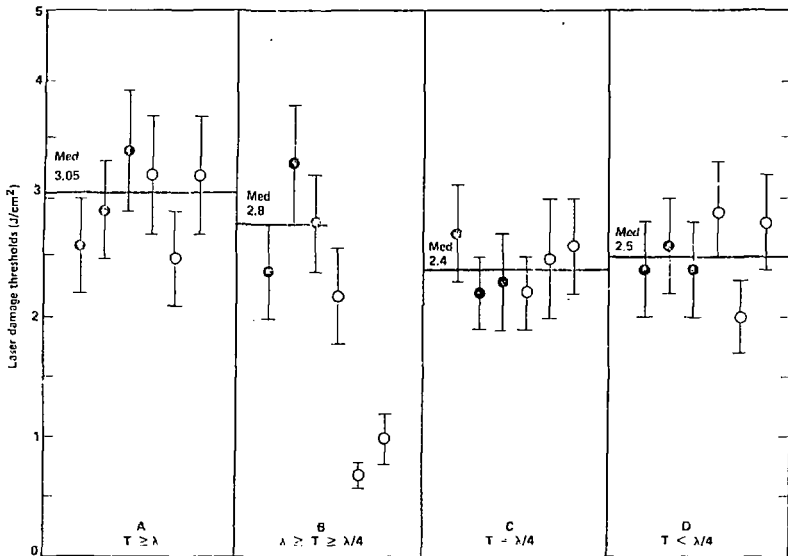


Figure 22. Laser-damage thresholds (355 nm, 0.6 ns) measured on four-layer Sc<sub>2</sub>O<sub>3</sub>/SiO<sub>2</sub> AR coatings as a function of the thickness layers used in the coatings. Data for three type-B coatings were neglected in determining the median because these coatings contained obvious flaws thought to have resulted from improper substrate cleaning.

Laser damage thresholds for these coatings are shown in Fig. 22. Filled circles indicate thresholds for coatings of each design that were made in the first deposition, and open circles are thresholds of coatings made in the second deposition. The median thresholds for the various designs, indicated by a horizontal bar, ranged from 2.4 to 3.1 J/cm<sup>2</sup>. This study showed little or no dependence of thresholds on layer thickness.

#### Acknowledgments

This paper reviews experiments which were designed and conducted with our colleagues at Optical Coating Laboratory, Inc.: C. K. Carniglia, T. Tuttle Hart, and T. L. Lichtenstein and at Lawrence Livermore National Laboratory: F. Rainer, M. C. Staggs, and C. L. Vercimak. Work performed under the auspices of the U.S. Department of Energy by Lawrence Livermore National Laboratory under Contract No. W-7405-ENG-48.

#### References

1. Rainer, F., Lowdermilk, W. H. and Milam, D., "Bulk and Surface Damage Thresholds of Crystals and Glasses at 248 nm," Opt. Eng., Vol. 22, pp. 431-434, 1983.
2. Dietz, R. W. and Bennett, J. M., "Bowl-feed Technique for Producing Supersmooth Optical Surfaces," Appl. Opt., Vol. 5, pp. 881-882, 1966.
3. Deaton, T. F. and Smith, W. L., "Laser-Induced Damage Measurements with 266 nm Pulses," Natl. Bur. Stand. (U.S.) Spec. Publ. 568, pp. 417-424, 1980.
4. Bennett, H. et al., "Ultraviolet Components for High Energy Applications," Naval Weapons Center Technical Publication 6015, Naval Weapons Center, China Lake, CA, March 1978.
5. Rainer, F., Lowdermilk, W. H., Milam, D., Tuttle Hart, T., Lichtenstein, T. L. and Carniglia, C. K., "Scandium Oxide Coatings for High-power UV Laser Applications," Appl. Opt., Vol. 21, pp. 3685-3688, 1982.
6. Carniglia, C. K., Apfel, J. H., Allen, T. H., Tuttle, T. A., Lowdermilk, W. H., Milam, D. and Rainer, F., "Recent Damage Results on Silica Titania Reflectors at 1 micron," Natl. Bur. Stand. (U.S.) Spec. Publ. 568, pp. 377-390, 1980.
7. Apfel, J. H., Enemark, E. A., Milam, D., Smith, W. L. and Weber, M. J., "The Effects of Barrier Layers and Surface Smoothness on 150-ps, 1.064-um Laser Damage of AR Coatings on Glass," Natl. Bur. Stand. (U.S.) Spec. Publ. 509, pp. 255-259, 1977.
8. Rainer, F., Lowdermilk, W. H., and Milam, D., "Damage Thresholds of Thin Film Materials and High Reflectors at 248 nm," Natl. Bur. Stand. (U.S.) Spec. Publ. 669, p. 274-281, 1984.
9. Newnam, B. E. and Gill, D. H., "Ultraviolet Damage Resistance of Laser Coatings," Natl. Bur. Stand. (U.S.) Spec. Publ. 541, pp. 190-201, 1978.
10. Walker, T. W., Guenther, A. H., Fray, C. G. and Nielsen, P., "Pulsed Damage Thresholds of Fluoride and Oxide Thin Films from 0.26um to 1.06um," Natl. Bur. Stand. (U.S.) Spec. Publ. 568, pp. 405-416, 1980.
11. Turner, A. F., "Ruby Laser Damage Thresholds in Evaporated Thin Films and Multilayer Coatings," Nat. Bur. Stand. (U.S.) Spec. Publ. 356, pp. 119-123, 1971.
12. Bettis, J. R., Guenther, A. H. and Glass, A. J., "The Refractive Index Dependence of Pulsed Laser Induced Damage," Nat. Bur. Stand. (U.S.) Spec. Publ. 414, pp. 214-218, 1974.
13. Staggs, M. C. and Rainer, F., "Damage Thresholds of Fused Silica, Plastics and KDP Crystals Measured with 0.6 ns, 355 nm Pulser," Natl. Bur. Stand. (U.S.) Spec. Publ. 1985 (in press).
14. Private communication: W. L. Smith, Sept. 1982. Also 1983 Laser Program Annual Report, Lawrence Livermore National Laboratory (in press).
15. Swain, J., Stokowski, S., Milam, D. and Rainer, F., "Improving the Bulk Damage Resistance of Potassium Dihydrogen Phosphate Crystals by Pulsed Laser Irradiation," Appl. Phys. Lett., Vol. 40, pp. 350-352, 1982.
16. Carniglia, C. K., Tuttle Hart, T., Rainer, F. and Staggs, M. C., "Recent Damage Results on High Reflector Coatings at 355 nm," Natl. Bur. Stand. (U.S.) Spec. Publ. (in press).
17. DeBell, G., Ph.D. Dissertation, Univ. of Rochester, University Microfilms, Ann Arbor, Mich. (1971).
18. Newnam, B. E. and Gill, D. H., "Laser Damage Resistance and Standing Wave Fields in Dielectric Coatings," J. Opt. Soc. Am., Vol. 66, pp. 166-, 1976.
19. Apfel, J. H., "Optical Coating Design with Reduced Electric Field Intensity," Appl. Opt., Vol. 16, pp. 1880-1885, 1977.
20. Tuttle Hart, T., Carniglia, C. K., Rainer, F. and Staggs, M. C., "Recent Damage Results for Antireflection Coatings at 355 nm," Natl. Bur. Stand. (U.S.) Spec. Publ., 1985 (in press).
21. Lowdermilk, W. H., Milam, D. and Rainer, F., "Damage to Coatings and Surfaces by 1.06um Pulses," Nat. Bur. Stand. (U.S.) Spec. Publ. 568, pp. 391-398, 1979.
22. Rainer, F., Vercimak, C. L., Milam, D., Carniglia, C. K. and Tuttle Hart, T., "Measurements of the Dependence of Damage Thresholds on Laser Wavelength, Pulse Duration and Film Thickness," Natl. Bur. Stand. (U.S.) Spec. Publ. 1985 (in press).

23. Newnam, B. E. and Gill, D. H., "Ultraviolet Damage Resistance of Laser Coatings," Nat. Bur. Stand. (U.S.) Spec. Publ. 541, pp. 190-201, 1978.
24. Newnam, B. E. and Gill, D. H., "Spectral Dependence of Damage Resistance of Refractory Oxide Optical Coatings," Nat. Bur. Stand. (U.S.) Spec. Publ. 462, pp. 292-300, 1981.
25. Walker, T. W., Guenther, A. H. and Nielsen, P. E., "Pulsed Laser-induced Damage to Thin-film Optical Coatings - Part I: Experimental," IEEE J. Quant. Elect., Vol. QE-17 (10), pp. 2041-2052, 1981.
26. Walker, T. W., Guenther, A. H. and Nielsen, P. E., "Pulsed Laser-induced Damage in Thin-film Optical Coatings - Part II: Theory," IEEE J. Quant. Elect., Vol. QE-17 (10), pp. 2053-2065, 1981.

#### DISCLAIMER

This document was prepared as an account of work sponsored by an agency of the United States Government. Neither the United States Government nor the University of California nor any of their employees, makes any warranty, express or implied, or assumes any legal liability or responsibility for the accuracy, completeness, or usefulness of any information, apparatus, product, or process disclosed, or represents that its use would not infringe privately owned rights. Reference herein to any specific commercial products, process, or service by trade name, trademark, manufacturer, or otherwise, does not necessarily constitute or imply its endorsement, recommendation, or favoring by the United States Government or the University of California. The views and opinions of authors expressed herein do not necessarily state or reflect those of the United States Government thereof, and shall not be used for advertising or product endorsement purposes.